Canadian Metallurgical Quarterly, Vol 46, No 3 pp 227-236, 2007

ANISOTROPIC CHARACTER OF TALC SURFACES AS REVEALED BY STREAMING POTENTIAL MEASUREMENTS, ATOMIC FORCE MICROSCOPY, MOLECULAR DYNAMICS SIMULATIONS AND CONTACT ANGLE MEASUREMENTS

J. NALASKOWSKI, B. ABDUL, H. DU and J.D. MILLER*

Department of Metallurgical Engineering, University of Utah,
Salt Lake City, UT 84112-0114, U.S.
*jdmiller@mines.utah.edu

(Received in revised form March, 2007)

Abstract — A study of the interfacial properties of the basal plane and the edge surfaces of talc is described in this paper. The isoelectric points measured at two different crystallographic surfaces by the streaming potential method were found to be similar and exist at about pH 3.0. In the case of the edge surface, the zeta potential increases at higher pH values which can be attributed to the hydration of surface magnesium ions. The forces between the edge of a 20 μm talc particle and the two different crystallographic surfaces of talc were measured at various pH values using atomic force microscopy (AFM). These measurements show differences between the properties of the basal plane and edge of the talc. Finally, the differences in the hydration of the basal plane and the edge of talc are revealed from molecular dynamics (MD) simulations. The basal plane of talc is much less hydrated than the edge as can be seen from the water density distribution functions which correlate quite well with the contact angle measurements at the basal plane surface and the edge surface. Improved quality of the edge surface was achieved by sandblasting (erosion with alumina) and research regarding the characteristics of this edge surface is in progress.

Résumé — On décrit dans cet article une étude des propriétés interfaciales de la surface du plan basal et des arêtes du talc. On a trouvé que les points isoélectriques mesurés à deux surfaces cristallographiques différentes par la méthode du potentiel électrocinétique étaient similaires et sont présents à un pH d'environ 3.0. Dans le cas de la surface de l'arête, le potentiel zêta augmente aux valeurs plus élevées de pH, ce que l'on peut attribuer à l'hydratation des ions magnésium de la surface. On a mesuré les forces entre l'arête d'une particule de talc de 20 μm et les deux différentes surfaces cristallographiques du talc à des valeurs variées du pH en utilisant la microscopie à force atomique (AFM). Ces mesures montrent les différences entre les propriétés du pland basal et de l'arête du talc. Finalement, on révèle les différences d'hydratation entre le plan basal et l'arête du talc par des simulations de dynamique moléculaire (MD). Le plan basal du talc est beaucoup moins hydraté que l'arête, tel qu'observé par les fonctions de distribution de densité de l'eau qui montrent une très bonne relation avec les mesures d'angle de contact à la surface du plan basal et à la surface de l'arête. On a obtenu une meilleure qualité de la surface de l'arête par sablage (érosion avec de l'oxyde d'aluminium) et la recherche concernant les caractéristiques de cette surface de l'arête est en cours.

INTRODUCTION

Phyllosilicate minerals, the sheet silicates, are important industrial minerals and include aluminum silicate minerals such as kaolinite, pyrophyllite and muscovite, as well as the corresponding magnesium silicate minerals, antigorite, talc and phlogopite. The most significant of the magnesium silicate minerals is talc, both as a valuable material in the paper, polymer, paint, lubricant, plastic, cosmetic and pharmaceutical industries, as well as an important gangue mineral in the flotation of various metal-bearing ores. In this regard the talc surface chemistry/physics is of particular interest to mineral processing engineers.

Talc, having a chemical formula $Mg_3(Si_4O_{10})(OH)_2$, is composed of three layers. Its middle layer is a brucite layer consisting of a magnesium-oxygen/hydroxyl octahedral, while the two outer layers are composed of silicon-oxygen tetrahedra. The brucite layer has the positive charge necessary to neutralize the two hexagonal networks of silica tetrahedra to give the crystal the sandwich structure and provide a neutral charge to the three-layer structure. These three-layer sheets are held together only by van der Waals forces so that

the layers are capable of slipping easily over one another which accounts for the soft character of the talc mineral. The basal surfaces of this elementary sheet do not contain hydroxyl groups or active sites which provide the basal plane of talc with a natural hydrophobicity and floatability. However, the edges of the talc particles are created by the breakage of the Si-O or Mg-O bonds and consequently the edges are expected to be hydrophilic.

Flotation of talc has been of interest to many researchers and substantial research has been reported [1-4]. It has been known in flotation practice that in addition to the primary cleavage along the basal plane, the edges may also play a significant role in terms of surfactant/depressant adsorption, bubble attachment and particle floatability. Also, the interaction and organization of the anisotropic talc particles is an important area of research and surface chemistry studies are in progress to determine the basis for the interaction of talc particles [5]. Efforts have been focussed to understand the surface chemistry of talc and other phyllosilicate minerals using titration, adsorption and electrophoretic measurements [6,7]. Generally, these experimental results reveal only the average behaviour of talc. Detailed experimental studies regarding the characteristics of the basal plane surface and the edge surface have been limited.

In this regard, the study of the anisotropic character of talc surfaces is now in progress. The results from streaming potential measurements, atomic force microscopy, molecular dynamics simulations and contact angle measurements are presented and discussed. The streaming potential method is well known but recent advances have made the study of flat mineral plates possible. The AFM colloidal probe technique has been successfully employed to study the interaction forces between particles and surfaces and has been extended to estimate the isoelectric point for specific crystallographic planes [8,9]. Molecular dynamics (MD) simulation is an extremely useful tool to generally explore the chemical and surface interactions and in this case to describe the structure of water at mineral surfaces. In the past decade, much research based on MD simulations has been reported for the study of water structures as well as the dynamic and thermodynamic characteristics of water/mineral systems [10-15].

EXPERIMENTAL

Materials

The talc sample used in this research was high quality white talc specimen from the collection of the Geology and Geophysics Department at the University of Utah. One talc sample was sliced parallel to the natural basal plane using a fine diamond saw, while the second sample was cut perpendicular to the basal plane. Both samples were gently polished using a diamond-encrusted polishing wheel. No visible diamond particles were observed under a scanning electron microscope (SEM) at the talc surface. Samples were cleaned before use by rinsing with methanol and Milli-Q water.

Additionally, a talc edge sample was sandblasted using a precision sand blasting machine – Pennwalt S.S White Airbrasive Unit Model-K. The abrasive medium (17.5 micron alumina powder) was discharged through a fine hand-held pen tool under high pressure on to the sample. The system was operated under the following conditions, pressure ~ 2.5 psi, nozzle size – 0.045 inch and the nozzle distance was held at ~5 cm from the sample surface. The blasted surface was then rinsed with deionized water, sonicated for 5 minutes to remove alumina particles from the surface and then imaged using the scanning electron microscope. The surface was compared with the surface of the unblasted sample.

Reagent grade KCl, HCl and KOH (Mallinckrodt) were used for ionic strength and pH control in streaming potential and AFM measurements. All solutions were prepared using water deionized and purified by Milli-Q Gradient A10 system (Millipore).

Methods

Scanning Electron Microscopy: Imaged talc surfaces and particles were mounted on a carbon tape and covered with a 20 nm thick gold layer using a Cressington Sputter 108 Auto Coater. Images of the particles were taken with a Hitachi S-3000N SEM using a secondary electron detector at a working distance of 27 mm and 15.0 - 20.0 keV of electron energy.

Streaming Potential: A commercial streaming potential analyzer (EKA, Brookhaven Instruments, Holtsville, NY) equipped with an asymmetric clamping cell was used to determine the ζ potential of sample surfaces. A schematic representation of the asymmetric clamping cell is shown in Figure 1. The cell comprises several parallel rectangular capillary channels formed by firmly pressing the test surface against a grooved spacer. At the two ends, the channels merge

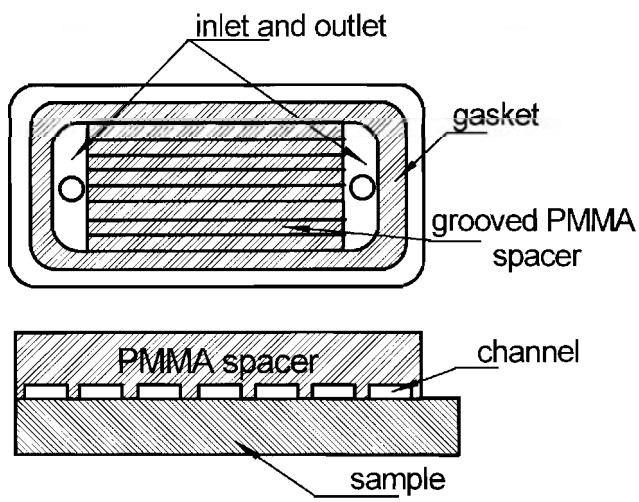

Fig. 1. Schematic representation of the asymmetric clamping cell and the geometric parameters defining a single capillary. Each channel has the following dimensions: length 20 mm; width 1.0 mm; height 0.14 mm.

into two common manifolds that act as the electrode compartments. The dimensions of a single rectangular channel are shown in Figure 1. Each rectangular capillary has a length L, width W and height h. While three of the sides of each capillary (channel) are made of a single material (the grooved spacer), the fourth side is the test substrate for which the streaming potential is sought.

In each experiment, the zeta potential was first determined for the PMMA (Polymethyl methacrylate) spacer/PMMA reference material and the zeta potential of PMMA (ζ_{PMMA}) was obtained. Next, the streaming potential was measured for the PMMA spacer/tested surface assembly and the average zeta potential ζ_{Avg} was obtained. Based on these measurements, the zeta potential of the tested sample ζ_{Test} was calculated using the formula [16]

$$\zeta_{Test} = 2\zeta_{Avg} - \zeta_{PMMA} \quad (1)$$

The experiments were done in a 1×10^{-3}M KCl background electrolyte and the pH was adjusted with HCl and KOH using the instrument's autotitrator unit.

Atomic Force Microscopy: Selected talc particles approximately 20 μm in size were glued with thermoplastic Epon 1001F resin (Shell) to the triangular silicon nitride AFM cantilevers (Veeco, Inc.) by means of an optical microscope and a micromanipulator. The scanning electron micrograph of the talc particle at the end of cantilever used for the measurements is shown on Figure 2.

Cantilevers with attached particles were gently rinsed with methanol and MilliQ water and were exposed to UV/O_3 (UV Cleaner, Bioforce Nanosciences) for 5 minutes prior to each experiment.

A PicoPlus AFM (Molecular Imaging, Inc.) was used for force measurements. Freshly cleaned talc plates (either base or edge surfaces) were placed in an open fluid cell filled with aqueous solution. A 100 μm closed loop scanner with maximum vertical range of 3 μm was used. Talc particles were glued to the triangular cantilever as mentioned previously. The measurements were done in a 1×10^{-3} M KCl background electrolyte and the pH was adjusted with HCl and KOH. After the solution was injected, the system was equilibrated for 15 minutes. The temperature during measurements was kept at 22 °C. For each concentration, at least 10 force measurements were taken at different locations on the talc surfaces. The spring constant of the cantilever was measured using the thermal noise method [17] and was found to be about 0.12 N/m. Measured deflection curves were converted to force versus separation distance curves using the SPIP software package.

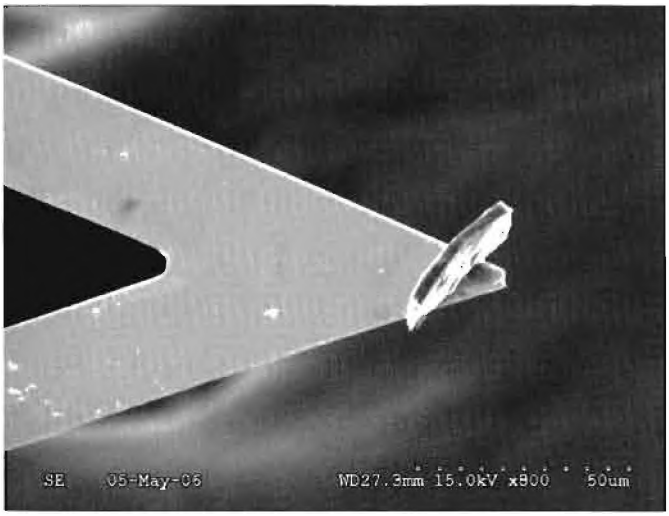

Fig. 2. SEM micrograph of talc particle glued to the AFM cantilever.

Molecular Dynamics Simulations: For the MD simulations, the DL_POLY_214 program was used [18]. A simple cubic cell containing water molecules and the desired talc mineral surface with periodic boundary conditions was used for the simulation. The simple point charge (SPC) water model [19] incorporated with the recently developed CLAYFF force field [20,21] was used for simulations. The intermolecular potential parameters are listed in Table I. The initial configuration of the talc mineral was constructed using lattice parameters provided by American Mineralogist Crystal Structure Database [22,23].

Initially, following the procedure previously reported [12,21,24,25] the talc crystal was simulated in an NPT assembly with the pressure fixed at 0.1 MPa and the temperature fixed at 300 K for 100 ps. After adding SPC water into the system, the simulation was performed in a NPT assembly using a Hoover thermostat [26]. The Leap-frog method with a time step of 1 fs was used to integrate the particle motion. A final simulation time of 1 ns (10^6 steps of 1 fs) including a 500 ps equilibration period was performed. The final results were analyzed based on the production of the 500 ps simulation after the equilibration period.

Contact Angle: Contact angles for water were measured on the talc surfaces using a Ramé-Hart goniometer and the sessile-drop technique for the cut/polished surfaces and both sessile-drop and captive bubble techniques in the case of cleaved face and cut/sandblasted edge surfaces. The water drop was placed on the surface and remained in contact with the needle of the microsyringe. The drop volume was

Table 1 – Potential parameters for water/water, water/ion interactions [20]

Species	σ_i(Å)	ε_i (kcal/mol)	Charge (q)
Water hydrogen	0	0	0.41
Hydroxyl hydrogen	0	0	0.425
Water oxygen	3.169	0.155	-0.82
Hydroxyl oxygen	3.169	0.155	-0.95
Bridging oxygen	3.169	0.155	-1.05
Apex oxygen	3.169	0.155	-1.2825
Silicon	3.706	1.8E-6	2.1
Magnesium	5.909	9E-7	1.36

increased and decreased until the three phase boundary moved over the surface. Both advancing and receding contact angles were measured as described in a previous contribution [27]. Reported values are the average values from measurements for drop diameters between 3 and 7 mm.

RESULTS AND DISCUSSION

SEM micrographs of the basal plane revealed that the talc surface is composed of terrace-like platelets. Although more flat areas on the sample surface were observed, the surface topography of the talc basal surface presented in Figure 3a was most typical for the sample used in this study.

The edge surface presented in Figure 3b exhibits a much finer structure. The platelets are still visible but their dimensions are much smaller than those observed on the basal plane. At a lower magnification, the layered structure of the talc sample was clearly visible. It can be speculated that the platelets visible on the SEM micrograph of the edge surface originate from the folding-over of talc edges or from the not exactly perpendicular cutting of the sample. The edge to the base plane ratio, however, is much greater on the edge surface than on the basal plane surface (Figure 3).

In addition to the SEM micrographs, both talc surfaces were characterized using AFM imaging with respect to the surface roughness. Both base and edge surfaces exhibit similar mean roughness values of approximately 100 nm as measured for the 625 μm^2 area. It can be expected that such high roughness and texture will have an influence on the subsequent streaming potential and interaction force measurements. Other procedures for the preparation of smoother talc edge surfaces have been considered. Specifically, the edge surface has been sandblasted and the results are presented in Figure 4.

For the talc edge surface presented in Figure 4a, the folding of the talc edges is clearly visible. This folding over seems to be taking place during the precision diamond saw cutting of the edges resulting in the contamination of the edge surface with basal platelets. For the talc edge surface presented in Figure 4b the layered structure of the talc edge surface is clearly visible. There is no contamination of alumina particles visible in the images even at higher magnifications. The surface was also analyzed for alumina contamination using EDS but no trace of alumina was found.

Hence, sand blasting with alumina abrasive seems to result in a comparatively finer edge surfaces, with an improved edge to basal plane ratio as desired for our surface chemistry studies and is therefore recommended in the preparation of edge surfaces. Further studies of the sandblasted edge surface are in progress. Some contact angle results are reported later in this paper, but most of the surface characteristics of the sandblasted edge surface are currently under study and will be reported in future publications.

Zeta potential values obtained from streaming potential measurements for both the cut basal plane and edge surfaces are presented as a function of pH in Figure 5. The isoelectric point (IEP) is observed around pH 3.0 for both base and edge surfaces.

The edge surface has more magnesium-oxygen/hydroxyl octahedral exposed to the solution which was expected to result in a higher IEP for this surface, similar to chrysotile which has magnesium on its surface layer and shows an IEP around pH 11.0. This was not observed in our measurements. However, in the case of the talc edge surface, the absolute value of the zeta potential significantly decreases at pH values higher than pH 6.0. This can be explained by the hydrolysis of magnesium ions [5]. At the higher values of pH, magnesium begins to hydrolyze and forms surface active $Mg(OH)^+$ ions which decrease the negative charge of the surface and at higher surface density may even render the talc surface positive.

Results from the AFM surface force measurements between a talc particle and base and edge surfaces of talc are

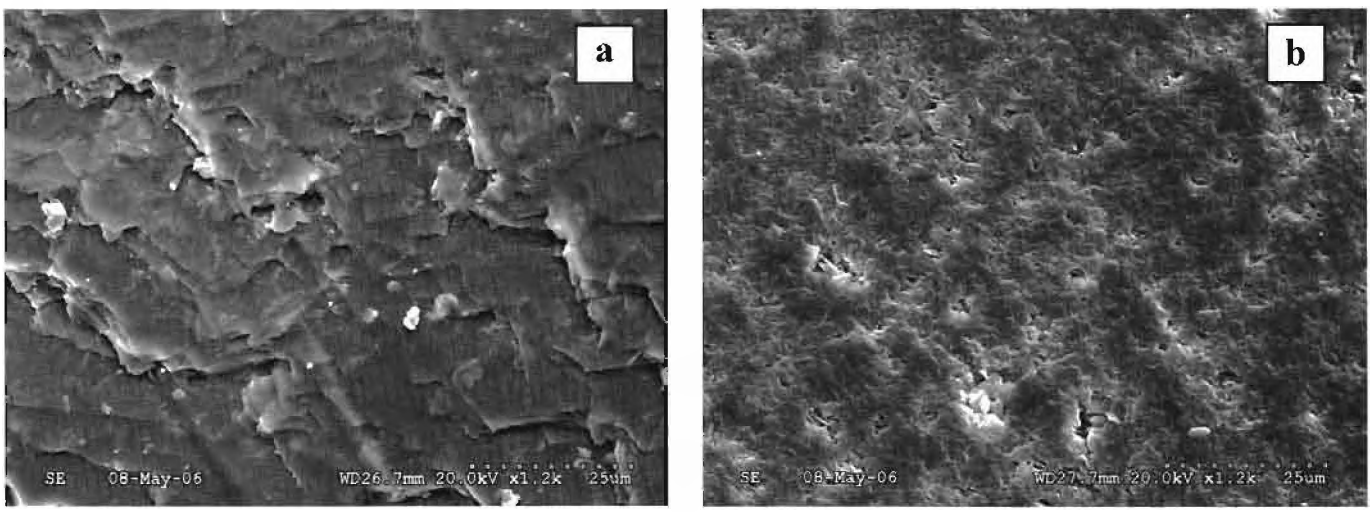

Fig. 3 . SEM micrographs of the basal plane a) and the edge plane b) surfaces of talc.

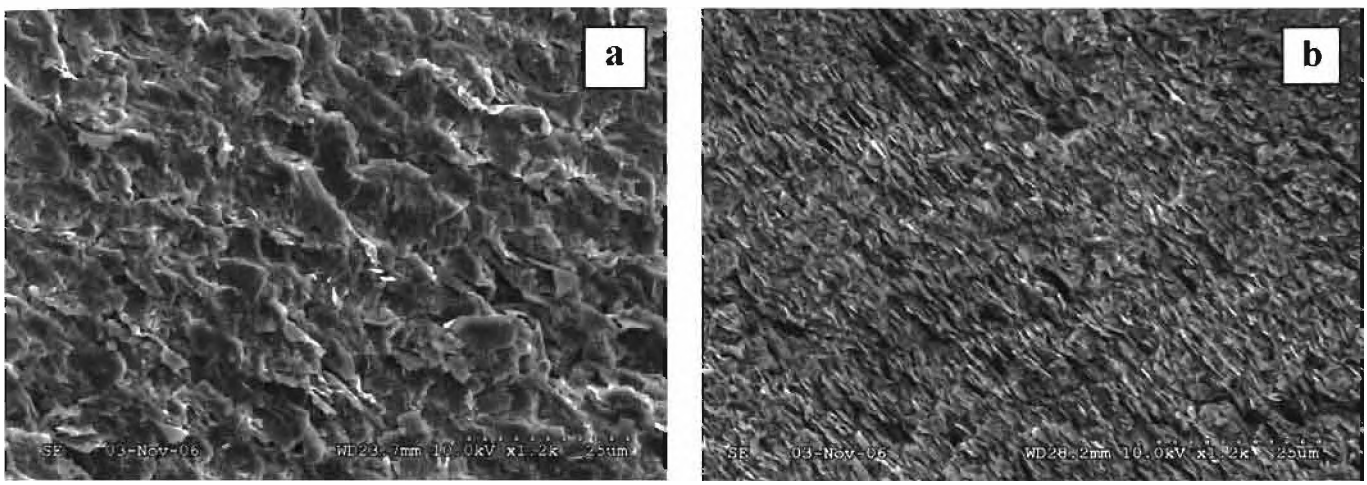

Fig. 4. SEM micrographs of the unblasted edge plane a) and blasted edge plane b) surface of talc.

presented in Figure 6. From the SEM micrograph of the talc particle attached to the AFM cantilever (Figure 2) it can be expected that the particle contacts the flat talc surface with its edge resulting in edge-base and edge-edge geometries. However, the actual area of contact is not well-defined (e.g. by reverse scanning procedure) due to the fragile nature of the cantilever-talc particle assembly. The possibility of the talc particle interacting with the surface at some angle to the basal plane cannot be completely ruled out at this time. Due to the ill-defined geometry of the interacting surfaces (particle position and roughness of the sample), the force curves can only be treated semi-quantitatively.

Measured interaction forces are of the DLVO type, exhibiting variations in range and magnitude of the electrical double layer (EDL) repulsion at separation distances greater than 5 nm and van der Waals attraction at separations below 5 nm. Existence of the hydration repulsion below 2 nm can also be postulated, especially for the more hydrated edge surface. However, there is a degree of uncertainty in the zero separation distance for these AFM measurements, especially when such rough surfaces are being studied.

The AFM results obtained correlate well with streaming potential measurements. In the case of the edge-base interaction, the lowest EDL repulsion is observed at pH 3.0. With an increase in pH, an increase in the magnitude of EDL repulsion is generally observed. The EDL repulsion in the case of the edge-edge geometry is small at the studied pH values, with the exception of pH 6 where the highest absolute value of the zeta potential was measured. The influence of magnesium hydrolysis and the decrease in the absolute zeta potential of the edge surface at higher pH is further confirmed by the force measurements.

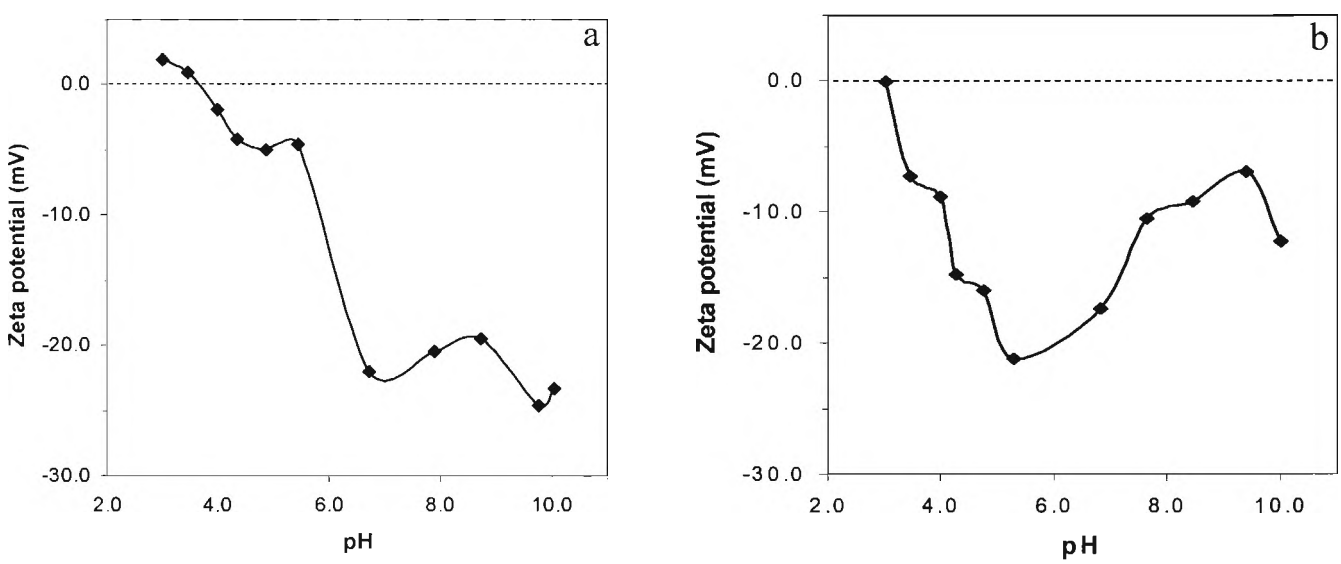

Fig. 5. Zeta potential at the basal plane surface of talc a) and the edge surface of talc b) as a function of pH.

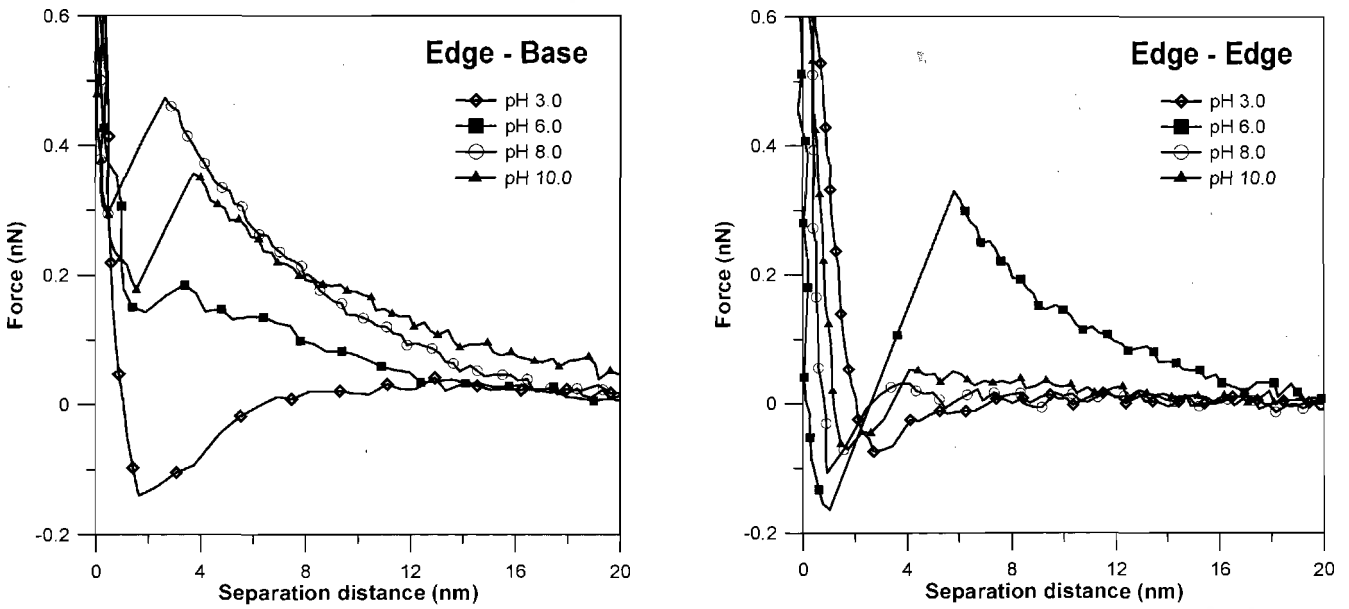

Fig. 6. Force curves for a talc particle interacting with base and edge surfaces of talc at different pH values.

Results from MD simulations of water interactions at the talc surfaces show the significant differences in hydration of these surfaces as seen in the snapshots of water molecules near the basal plane surface and the edge surface of talc presented in Figure 5. It is clear that, when interacting with the basal plane, there exists a gap between the water phase and the talc, reflecting the dominance of the so-called "excluded volume" or "hard wall" effect for this system [28, 29]. This is due to the absence of specific hydrogen bonding donor and/or acceptor sites on the basal plane of talc and the week interaction between water molecules and the basal plane.

Figure 7a shows the structure of water at the (001) basal plan, Figures 7b and 7c reveal the water structures at the talc edges orthogonal to the (001) plane. The large dark grey balls represent the oxygen atoms in the talc mineral and the small dark grey balls represent the water oxygen. The large white balls are silicon atoms, the large light grey balls are magnesium atoms and small white balls are water hydrogen atoms.

The relatively weak water/talc interaction on the molecular scale is the origin of the macroscopic hydrophobic character of talc. In contrast, water molecules are tightly bonded with atoms on the edge surface of talc indicated by the close contact between the water phase and the edge surface as seen in Figure 7b and 7c. The existence of electron donor/acceptor sites at the edge facilitates the formation of strong hydrogen bonds and wetting of the hydrophilic edges.

The water density distribution functions along normals to the talc surfaces are plotted in Figures 8a and 8b for the basal plane and edge surface respectively. As expected, due to the natural hydrophobicity of the talc basal plane, water molecules are expelled from the surface. Similarly to previous reports in the literature [30,31], the primary water density peak is located at about 3.1 Å away from the surface, a distance which is significantly larger than the distance between the hydrogen bonded water/water molecules, approximately 2.8 Å [32-37]. This observation reveals the weak interaction between the water molecules and talc basal plane. On the other hand, water molecules interact strongly with atoms at the edge of the talc crystal as indicated by the small distance between water molecules and the talc edge. Also, due to the complex structure of the talc edge, some water molecules can even be accommodated into the top layer of the crystal lattice as indicated by the noticeable zero distance water density. The complexity of the edge surface explains the more complicated peaks of the water density distribution function as well.

The water dipole distribution function provides more detailed information regarding the molecular interaction between the water molecules and surface atoms in the crystal. As seen in Figure 9a, interfacial water molecules are orientated preferentially parallel to the talc basal plane which can be directly explained by the absence of hydrogen bonding donor/acceptor sites. In contrast, as shown in Figure 9b, when near the talc edge, the orientations of water molecules are dominated by the hydrogen bonding structures. When surface oxygen atoms participate in hydrogen bonding, interfacial water dipoles are pointing toward the surface and when magnesium/silicon atoms interact with the water molecules, the interfacial water dipoles are pointing away from the surface. The large interfacial water density and the exclusive orientation of water dipoles of either close to 180° or close to 0° reflect the strong interactions between water and the talc edge surface, thus leading to the expectation that the talc edge should be hydrophilic.

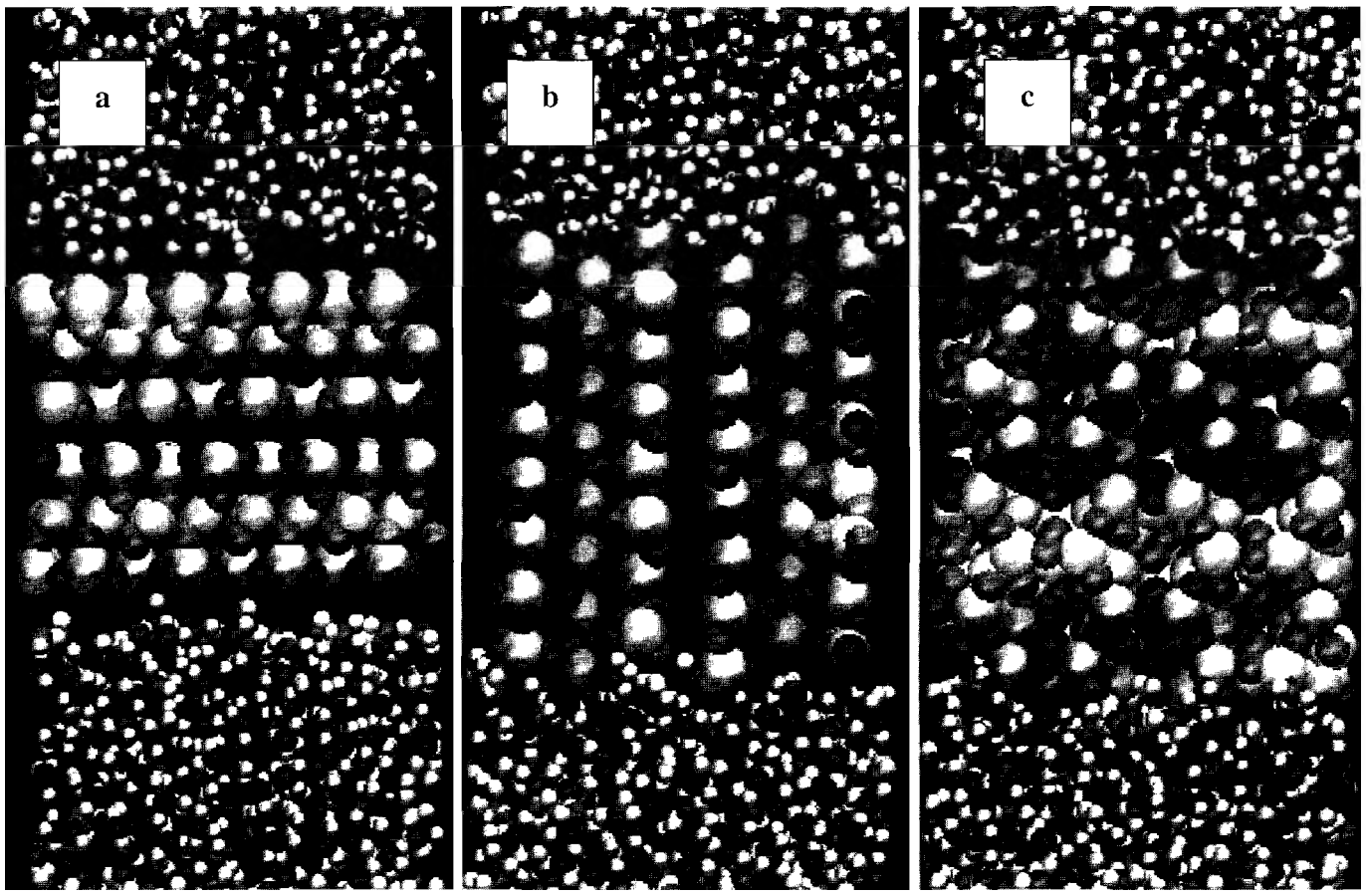

Fig. 7. MD simulation snapshots of equilibrated water at talc surfaces.

These differences in the interfacial water structure between the basal plane and edge surfaces were confirmed by the contact angle measurements for the cut and polished surfaces. For the basal plane surface used in this study, the advancing water contact angle was θ_A=72°, while for the edge surface, the advancing water contact angle was θ_A=57°. Receding contact angles (θ_R) for both surfaces were similar and lower than 5°. Such a great contact angle hysteresis is caused by the significant roughness and heterogeneity at the talc surface. The more hydrophobic character of the talc base is, however, clearly visible. Other samples of talc measured in our laboratory exhibited an even greater difference between wettability of the basal plane surface (θ_A=64° and θ_R=31°) and the edge surface (θ_A=31° and θ_R=9°).

Contact angle measurements were also done for a freshly cleaved basal plane surface and a precision cut edge surface using both the sessile drop technique and the captive bubble technique. For the freshly cleaved basal plane surface, the advancing sessile drop contact angle was θ_A=62 ± 5°, while for the edge surface, the advancing water contact angle was θ_A=48 ± 3°. Receding contact angles (θ_R) for both surfaces were similar and lower than 5°. Contact angle values obtained by the captive bubble technique were about θ=48 ± 4° for the freshly cleaved basal plane surface and θ=23 ± 2° for the edge surface which are comparable to the values obtained by other researchers [38].

In contrast, for the captive bubble measurements at the edge surface, the bubble did not attach to the sandblasted edge surface and a contact angle of zero was observed in most cases. The contact angle by sessile drop was less than 10°. These results are expected because the sandblasted (alumina eroded) edge surface is of higher quality with respect to contamination with basal plane platelets (Figure 4).

CONCLUSIONS

While the streaming potential measurements have shown similar IEP for both the cut and polished surfaces (pH ~ 3), the influence of magnesium hydrolysis at the edge surface at higher pH values is clearly revealed. Interaction forces measured between the talc particle edge and the basal plane and edge surfaces have shown further differences between these surfaces and were in good agreement with results from streaming potential measurements. There is still some concern regarding surface preparation and efforts continue to improve the quality of base and edge surfaces for further study.

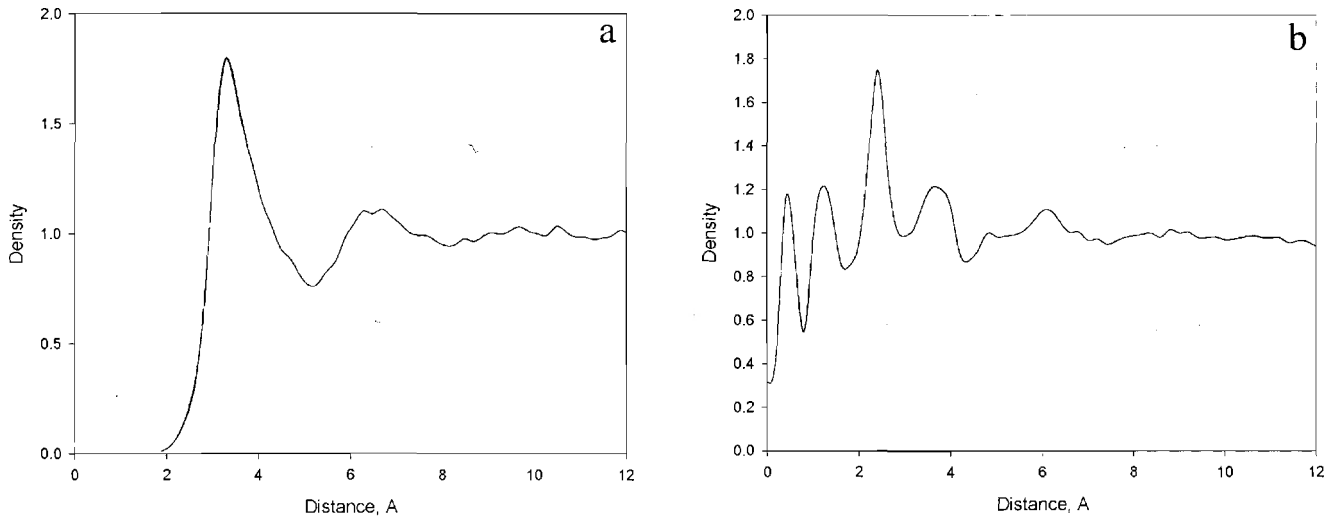

Fig. 8. Interfacial water density distribution function at the talc basal plane surface a) and the talc edge surface b).

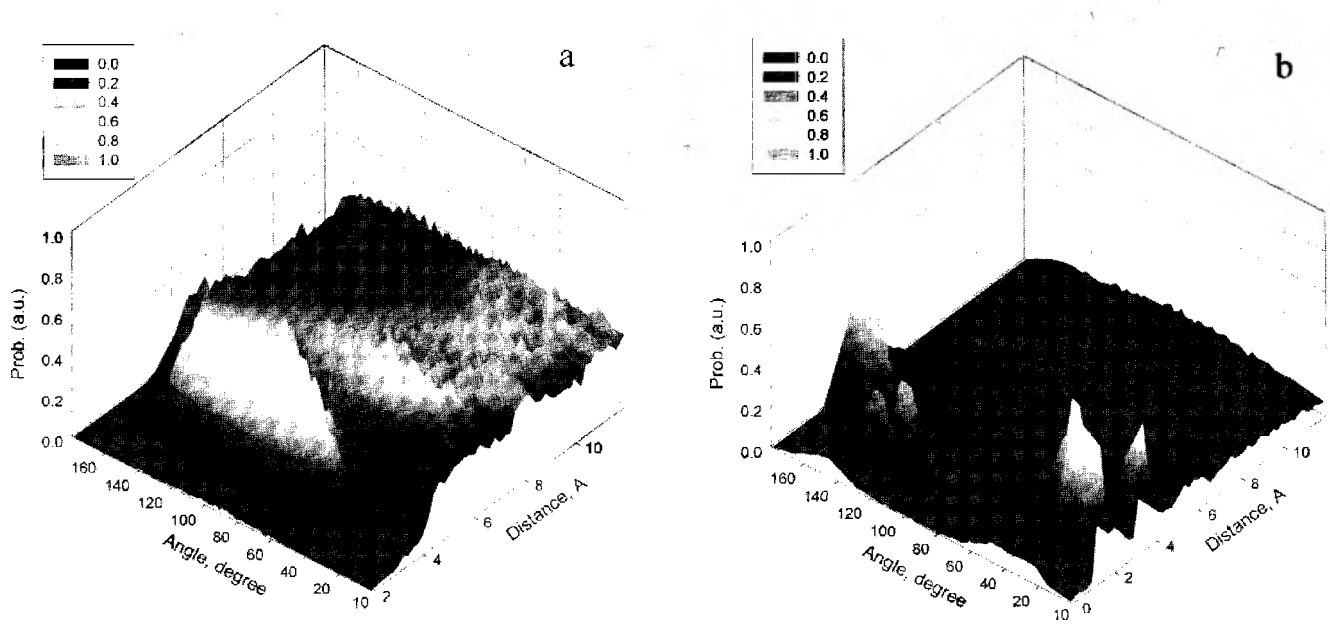

Fig. 9. Interfacial water dipole moment distribution function at the talc basal plane a) and the talc edges b).

MD simulations of water structures at the basal plane and edge surfaces of talc provide detailed information regarding the interaction between water molecules and crystal atoms at the talc surfaces. Due to the absence of electron donor/acceptor sites at the talc basal plane, water molecules interact weakly with the surface atoms and arrange themselves randomly in the vicinity of the surface. On the other hand, the exposed oxygen/magnesium/silicon atoms at the edge surface provide abundant hydrogen bonding sites, therefore, most importantly, interfacial water dipoles are orientated either away from or toward the edge surface. This strong hydrogen bonding ability of edge atoms explains the hydrophilic character of the talc edge. These results are in accord with the water contact angle measurements which clearly demonstrate the more hydrophilic character of the talc edge surface.

Finally, the contact angle results confirmed the MDS analysis. Experimental results for the cut and polished surfaces are contrasted to the results for a cleaved basal plane surface and a cut edge surface. In addition, preparation of a sandblasted (alumina eroded) edge surface resulted in a more ideal state for the edge surface with the presence of only a few basal plane platelets and clearly revealed the hydrophilic character of the edge surface.

ACKNOWLEDGEMENTS

Financial support provided by the Department of Energy, Basic Science Division Grant No. DE-FG-03-93ER14315 is gratefully acknowledged. In addition, this study was prompted to some extent by collaborative research supported by NSF under grant Nos. INT-0227583 and INT-0352807. Although the research described in this article has been funded partially by these agencies, it has not been subjected to their peer and policy review and therefore does not necessarily reflect the views of these agencies and no official endorsement should be inferred.

REFERENCES

1. R.K. Rath, S. Subramanian and J.S. Laskowski, "Adsorption of Dextrin and Guar Gum onto Talc. A Comparative Study", *Langmuir*, 1997, vol. 13(23); pp. 6260-6266.
2. S. Kelebek, "Wetting Behavior, Polar Characteristics and Flotation of Inherently Hydrophobic Minerals", *Transactions. Mining &. Metall. (Section C: Mineral Process. & Extr. Metall.)*, 1987, vol. 96, pp. 103-107.
3. M.C. Fuerstenau, A. Lopez-Valdieso and D.W. Fuerstenau, "Role of Hydrolyzed Cations in the Natural Hydrophobicity of Talc", *Int. J. Miner. Process.*, 1988, vol. 23, pp. 161-170.
4. H. Du and J.D. Miller, "A Molecular Dynamic Study of Water Structure and Adsorption States at Talc Surfaces", accepted for publication in *International Journal of Mineral Processing*, 2007.
5. K.E. Bremmell and J. Addai-Mensah, "Interfacial-chemistry Mediated Behavior of Colloidal Talc Dispersions", *J. Colloid Interface Sci.*, 2005, vol. 283(2), pp. 385-391.
6. G. Maelhammar, "Determination of Some Surface Properties of Talc", *Colloids Surf.*, 1990, vol. 44, pp. 61-69.
7. E. Steenberg and P.J. Harris, "Surface-chemical and Mineralogical Properties Relevant to the Flotation of Talc and Other Layer Silicates", *Extractive Metallurgy*, 1985, No. 209, p. 22.
8. S. Veeramasuneni, M.R. Yalamanchili and J.D. Miller, "Measurement of Interaction Forces between Silica and Alpha-alumina by Atomic Force Microscopy", *J. Colloid Interface Sci.*, 1996, vol. 184(2), pp. 594-600.
9. S. Assemi, J. Nalaskowski, J.D. Miller and W.P. Johnson, "Isoelectric Point of Fluorite by Direct Force Measurements Using Atomic Force Microscopy", *Langmuir*, 2006, vol. 22(4), pp. 1403-1405.
10. S.H. Lee and P.J. Rossky, "A Comparison of the Structure and Dynamics of Liquid Water at Hydrophobic and Hydrophilic Surface-A Molecular Dynamics Simulation Study", *J. Chem. Phys.*, 1994, vol. 100, pp. 3334-3345.
11. J.R. Rustad, A.R. Felmy and E.J. Bylaska, "Molecular Simulation of the Magnetite-water Interface", *Geochimica et Cosmochimica Acta*, 2003, vol. 67, pp. 1001-1016.
12. A.G. Kalinichev and R.J. Kirkpatrick, "Molecular Dynamics Modeling of Chloride Binding to the Surfaces of Ca Hydroxide, Hydrated Ca-aluminate and Ca-Silicate Phases", *Chemistry of Materials*, 2002, vol. 14, pp. 3539-3549.
13. E. Soper, C. Hartnig, P. Gallo and M. Rovere, "Water in Porous Glasses. A Computer Simulation Study", *Journal of Molecular Liquids*, 1999, vol. 80, pp. 165-178.
14. J.R. Rustad, "Molecular Models of Surface Relaxation, Hydroxylation and Surface Charging at Oxide-water Interfaces", *Reviews in Mineralogy and Geochemistry*, 2001, vol. 42, pp. 169-197.
15. P. Gallo, M. Rapinesi and M. Rovere, "Confined Water in the Low Hydration Regime", *J. Chem. Phys.*, 2002, pp. 369-375.
16. S.L. Walker, S. Bhattacharjee, E.M.V. Hoek and M. Elimelech, "A Novel Asymmetric Clamping Cell for Measuring Streaming Potential of Flat Surfaces", *Langmuir*, 2002, vol. 18(6), pp. 2193-2198.
17. R. Levy and M. Maaloum, "Measuring the Spring Constant of Atomic Force Microscope Cantilever: Thermal Fluctuations and Other Methods", *Nanotechnology*, 2002, vol. 13, pp. 33-77.
18. T. Forester, and W. Smith, *DL_POLY User Manual*, No., 1995.
19. H.J.C. Berendsen, J.R. Grigera and T.P. Straatsma, "The Missing Term in Effective Pair Potentials", *J. Phys. Chem.*, 1987, vol. 91(24), pp. 6269-71.
20. R.T. Cygan, J.J. Liang and A.G. Kalinichev, eds. "Molecular Models of Hydroxide, Oxyhydroxide and Clay Phases and the Development of a General Force Field", *J. Chem. Phys. B*, 2004, vol. 108, pp. 1255-1266.
21. R.T. Cygan, "Molecular Modeling in Mineralogy and Geochemistry", *Reviews in Mineralogy and Geochemistry*, 2001, vol. 42, pp. 1-35.
22. J.W. Gruner, *The Crystal Structures of Talc and Pyrophyllite*, 1934.
23. B. Perdikatsis and H. Burzlaff, "Strukturverfeinerung am talk $Mg_3[(OH)_2Si_4O_{10}]$", *Zeitschrift fur Kristallographie*, 1981, vol. 156, pp. 177-186.
24. R.J. Kirkpatrick, A.G. Kalinichev, J. Wang, X. Hou and J.E. Amonette, "Molecular Modelling of the Vibrational Spectra of Interlayer and Surface Species of Layered Double Hydroxides", *The Application of Vibrational Spectroscopy to Clay Minerals and Layered Double Hydroxides*, 2005, CMS Workshop Lectures, vol. 13, pp. 239-285.
25. H.J.C. Berendsen, J.P.M. Postma, W.F. Van Gunsteren and J. Hermans, "Interaction Models for Water in Relation to Protein Hydration", *Jerusalem Symposia on Quantum Chemistry and Biochemistry*, 1981, vol. 14, pp. 331-342.
26. S. Melchionna, G. Ciccotti and B.L. Holian, "Hoover NPT Dynamics for Systems Varying in Shape and Size", *Molecular Physics*, 1993, vol. 78(3), pp. 33-544.
27. J. Drelich, J.D. Miller and R.J. Good, "The Effect of Drop (Bubble) Size on Advancing and Receding Contact Angles for Heterogeneous and Rough Solid Surfaces as Observed with Sessile-drop and Captive-bubble Techniques", *J. Colloid Interface Sci.*, 1996, vol. 179(1), pp. 37-50.
28. F.F. Abraham, "The Interfacial Density Profile of a Lennard-Jones Fluid in Contact with a (100) Lennard-Jones Wall and Its Relationship to Idealized Fluid/wall Systems: A Monte Carlo Simulation", *J. Chem. Phys.*, 1978, vol. 68, pp. 3713-3716.
29. C.J. Yu, A.G. Richter, A. Datta, M.K. Durbin and P. Dutta, "Observation of Molecular Layering in Thin Liquid Films Using X-ray Reflectivity", *Phys. Rev. Letters*, 1999, vol. 82, pp. 2326-2329.
30. J. Wang, A.G. Kalinichev and R.J. Kirkpatrick, "Molecular Dynamics Modeling of the 10-A Phase at Subduction Zone Conditions", *Earth and Planetary Science Letters*, 2004, vol. 222, pp. 517-527.
31. J. Wang, A.G. Kalinichev and R.J. Kirkpatrick, "Molecular Modeling of Water Structure in Nano-pores Between Brucite (001) Surfaces", *Geochimica et Cosmochimica Acta*, 2004, vol. 68, pp. 3351-3365.
32. S.H. Lee and J.C. Rasaiah, "Molecular Dynamics Simulation of Ionic Mobility.I. Alkali Metal Cations in Water at 25 C", *J. Chem. Phys.*, 1994, vol. 101(8), pp. 1994, 6964.
33. J.C. Rasaiah, J. Zhu and S.H. Lee, "Solvent Effects in Weak Electrolytes. I. Effect of a Hard Sphere Solvent on the Sticky Electrolyte Model with L = s", *J. Chem. Phys.*, 1990, vol. 92(7), pp. 1990, 4636.
34. R.M. Lynden-Bell and J.C. Rasaiah, "From Hydrophobic to Hydrophilic Behaviour: A Simulation Study of Solvation Entropy and Free Energy of Simple Solutes", *J. Chem. Phys.*, 1997, vol. 107(6), p. 1982.
35. L.X. Dang, J.E. Rice, J. Caldwell and P.A. Kollman, "Ion solvation in Polarizable Water: Molecular Dynamics Simulations", *JACS*, 1991, vol. 113(7), pp. 2481-2486.
36. L.X. Dang, J.E. Rice and P.A. Kollman, "The Effect of Water Models on the Interaction of the Sodium-chloride Ion Pair in Water: Molecular Dynamics Simulations", *J. Chem. Phys.*, 1990, vol. 93(10), pp. 7528-7529.
37. L.X. Dang and B.M. Pettitt, "Chloride Ion Pairs in Water", *JACS*, 1987, vol. 109(18), pp. 5531-5532.
38. D.W.Fuerstenau and P.Huang, "Interfacial Phenomena Involved in Talc Flotation and Depression", *Proceeding of XXII International Mineral Processing Congress*, Sept. 29-Oct. 3, 2003, Cape Town, South Africa,